Analysis and computation of the acoustic scattering by an elastic prolate spheroid obtained from the *T*-matrix formulation

Lawrence Flax and Louis R. Dragonette

Naval Research Laboratory, Washington, DC 20375

V. K. Varadan and V. V. Varadan

Wave Propagation Group, Department of Engineering Mechanics, The Ohio State University, Columbus, Ohio 43210

(Received 18 August 1981; accepted for publication 8 January 1982)

The *T*-matrix formulation is used to compute the form function of an elastic prolate spheroid. The method allows acoustic scattering computations to be made for finite bodies at frequencies into the resonance region, and the lowest order resonance observed is, as expected, due to the excitation of a Rayleigh surface wave.

PACS numbers: 43.20.Fn, 43.30.Gv, 68.25. + j, 43.20.Bi, 43.20.Tb

INTRODUCTION

The excitation of the natural modes of vibration of a submerged target has a strong influence on the steady-state response of the target to an incident plane acoustic wave.[1-4] An analytical formulation of scattering behavior in terms of separate geometric and resonance terms was given by Flax *et al.*[4] The formulation was applied to solid metal spheres and infinite cylinders. For targets fabricated of materials whose density and sound speeds are larger than the density and sound speed in the surrounding fluid, the acoustic response of the target can be described in terms of a background of rigid body scattering onto which the resonances are superimposed.[4] For hollow targets, the appropriate geometric background term ranges from soft or Dirichlet boundary conditions for small frequency (ν) thickness (d) products to a rigid body background term at high νd values.[5] Extensive use has been made of resonance theory in acoustic problems which involve planar, infinite cylindrical, and spherical geometries. A summary of this previous work and an extensive reference list can be found in Ref. 6.

In this paper a solution is developed for the scattering by an elastic prolate spheroid in water, and results are compared with predictions made from resonance considerations. The scattering by an elastic prolate spheroid has been formulated in terms of an expansion in spheroidal wave functions,[7] but no elastic scattering computations have been made from that formulation because of complexity in the use of spheroidal functions as well as the difficulty in matching boundary conditions. Computations have been made in terms of spheroidal functions, for spheroids which satisfy rigid or soft boundary conditions, at end on incidence,[8-10] and approximate methods to describe the scattering by rigid and soft spheroids at arbitrary incidence angles have also been considered.[11-13]

The *T*-matrix formulation, utilized in this work, allows an expansion, in terms of spherical basis functions,[14-18] of the scattering by an elastic prolate spheroid. The method has been used successfully to describe the scattering by an elastic finite cylinder,[18] as was demonstrated by comparison with experimental measurements. The *T* matrix has also been applied by the present authors to the case of monostatic and bistatic scattering by rigid prolate spheroids[19] and those results compared favorably with the predictions of simple geometric scattering models. The computations made here are compared with predictions made from resonance response considerations.

I. THEORY

The geometry of the problem under consideration is described in Fig. 1. An elastic prolate spheroid with a semi-major axis, a, and a semi-minor axis, b, is illuminated, by a plane acoustic wave of circular frequency ω and wavenumber k_f along the major axis.

The displacement vector corresponding to the incident wave is denoted by $\mathbf{U}^i$ and that corresponding to the scattered wave $\mathbf{U}^s$. The displacement vector in the elastic medium is denoted by $\mathbf{U}$. Since the incident wave has time dependence $\exp(-i\omega t)$, all field quantities will have the same frequency, so that the time factor is henceforth suppressed.

The total displacement field $\mathbf{U}_f$ in the fluid is given by

$$\mathbf{U}_f(r)=\mathbf{U}^i(r)+\mathbf{U}^s(r), \tag{1}$$

where r is the position vector of the field point. The equation of motion for $\mathbf{U}_f$ is then

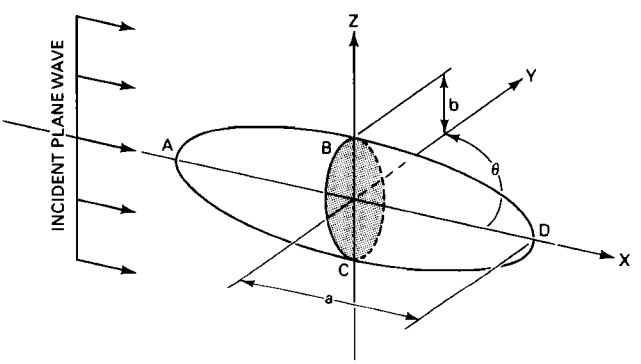

FIG. 1. The geometry of the problem.

$$\nabla \cdot \mathbf{T}_f + \rho_f \omega^2 \mathbf{U}_f = 0, \tag{2a}$$

where $\mathbf{T}_f$ is the stress tensor related to the displacement by

$$\mathbf{T}_f = \mathbf{I}\lambda_f \nabla \cdot \mathbf{U}_f, \tag{2b}$$

I is the idemfactor and λ_f the Lamé constant. The surface traction for the fluid is defined as

$$\mathbf{t}_f = \hat{n} \cdot \mathbf{T}_f = \mathbf{T}_f \cdot \hat{n}, \tag{2c}$$

where $\hat{n}$ is the outward normal to the surface.

The Green's displacement, $\mathbf{G}_f$, and stress tensor, $\boldsymbol{\Sigma}_f$, corresponding to Eqs. [(2a)–(2c)] are defined by

$$\nabla \cdot \boldsymbol{\Sigma}_f + \rho_f \omega^2 \mathbf{G}_f = -\mathbf{I}\delta(r - r') \tag{3a}$$

and

$$\boldsymbol{\Sigma}_f(r, r') = \lambda_f \mathbf{I} \nabla \cdot \mathbf{G}_f, \tag{3b}$$

where r is the position vector of a field point and r' the source point. These quantities are third rank tensors.

The equation describing the stress tensor in the elastic body is

$$\mathbf{T} = \mathbf{I}\lambda \nabla \cdot \mathbf{U} + \mu(\nabla \mathbf{U} + \mathbf{U}\nabla). \tag{4a}$$

The Green's displacement and stress tensor corresponding to Eq. (4a) are given by

$$\nabla \cdot \boldsymbol{\Sigma} + \rho\omega^2 \mathbf{G} = -\mathbf{I}\delta(r - r'), \tag{4b}$$

$$\boldsymbol{\Sigma} = \mathbf{I}\lambda \cdot \mathbf{G} + \mu(\nabla \mathbf{G} + \mathbf{G}\nabla). \tag{4c}$$

The surface traction is once again $t = \hat{n} \cdot \mathbf{T}$ and λ and μ are the Lamé constants of the body. When $\mu = 0$, these equations reduce to the fluid case.

The boundary conditions on the surface S between the fluid and the elastic obstacle are

$$\hat{n} \cdot \mathbf{U}_f = \hat{n} \cdot \mathbf{U}, \tag{5a}$$

$$\hat{n} \cdot \mathbf{t}_f = \hat{n} \cdot \mathbf{t}, \tag{5b}$$

$$(\hat{n} \cdot \mathbf{t})_{\tan} = 0, \tag{5c}$$

at the surface of the boundary.

The analytical properties and theoretical formulation of the T matrix have been discussed in Refs. 15–18. The starting point is the integral representation of the displacement field inside and outside the boundary S of the scatterer. The integral representation (see Ref. 16) is given for the fluid region as

$$\mathbf{U}^i(r) + \int_S \{\mathbf{U}_f'[\hat{n} \cdot \boldsymbol{\Sigma}(r, r')] - \mathbf{t}_f' \cdot \mathbf{G}_f(r, r')\} dS'$$
$$= \mathbf{U}_f(r); \quad r \text{ outside } S$$
$$= 0; \quad r \text{ inside } S. \tag{6a}$$

For the solid

$$-\int_S \{\mathbf{U}' \cdot [\hat{n} \cdot \boldsymbol{\Sigma}(r, r')] - \mathbf{t}' \cdot \mathbf{G}(r, r')\} dS'$$
$$= \mathbf{U}(r); \quad r \text{ inside } S$$
$$= 0; \quad r \text{ outside } S. \tag{6b}$$

In Eqs. (6a) and (6b), the primes on $\mathbf{U}$, $\mathbf{U}_f$, etc. indicate that they are functions of r' a point on S, and dS' is an element of area on S centered at r'.

II. T MATRIX FOR A SOLID IN A FLUID

For elastic waves in a three-dimensional medium, the total motion may be decomposed into three parts: $\psi_{1\sigma mn}$, $\psi_{2\sigma mn}$, and $\psi_{3\sigma mn}$. The $\psi_{1\sigma mn}$ is the vector basis function representing the longitudinal motion propagating with speed c_1 and wavenumber k_1; $\psi_{2\sigma mn}$ and $\psi_{3\sigma mn}$ are the two components of the transverse field in the solid with speeds c_s and wavenumber k_s. In spherical coordinates (r, θ, ϕ) the basis functions are

$$\boldsymbol{\psi}_{1\sigma mn} = (k_1/k_s)^{1/2} \epsilon_{mn} \nabla[h_n(k_1 r) Y^{\sigma}_{mn}(\theta, \phi)], \tag{7a}$$

$$\boldsymbol{\psi}_{2\sigma mn} = k_s \eta_{mn} \nabla \times [\mathbf{r} h_n(k_s r) Y^{\sigma}_{mn}(\theta, \sigma)], \tag{7b}$$

and

$$\boldsymbol{\psi}_{3\sigma mn} (1/k_s) \nabla \times \boldsymbol{\psi}_{2\sigma mn}. \tag{7c}$$

The basis functions in the fluid region, which represent longitudinal motion propagating with speed c and wavenumber k, are

$$\psi_{f\sigma mn} = \epsilon_{mn} \nabla[h_n(kr) Y^{\sigma}_{mn}(\theta, \phi)]. \tag{7d}$$

In the above equations, h_n is the spherical Hankel function of the first kind. The Y^{σ}_{mn} are the spherical surface harmonics where σ specifies azimuthal parity, m specifies rand, and n specifies the order of the harmonics,

$$Y^1_{mn}(\theta, \phi) = P^m_n(\cos\theta) \cos m\phi \text{ even parity},$$
$$Y^2_{mn}(\theta, \phi) = P^m_n(\cos\theta) \sin m\phi \text{ odd parity}. \tag{8}$$

The normalization constant ϵ_{mn} and η_{mn} are defined by

$$\epsilon_{mn} = \left(\frac{\epsilon_m (2n+1)(n-m)!}{4\pi(n+m)!}\right)^{1/2}, \quad \epsilon_0 = 1, \quad \epsilon_m = 2;\ m > 0 \tag{9a}$$

and

$$\eta_{mn} = \epsilon_{mn}/[n(n+1)]^{1/2}. \tag{9b}$$

For brevity, we abbreviate the basis function in the solid as

$$\boldsymbol{\psi}_{1\sigma mn}, \boldsymbol{\psi}_{2\sigma mn}, \boldsymbol{\psi}_{3\sigma mn} = \boldsymbol{\psi}_{\nu n}, \quad \nu = 1, 2, 3$$

and in the fluid as

$$\boldsymbol{\psi}_{f\sigma mn} = \boldsymbol{\psi}_{fn}.$$

The wave function above satisfies the radiation condition at infinity. In order to expand fields that are finite at the origin, one replaces the Hankel function h_n by the spherical function j_n. Throughout this paper a boldface symbol with a caret indicates the real part of the function.

The scattered field $\mathbf{U}^s$ must satisfy the radiation condition at infinity and hence is expanded with spherical Hankel functions

$$\mathbf{U}^s(r) = \sum f_n \boldsymbol{\psi}_{fn}. \tag{10a}$$

The incident field $\mathbf{U}^i$ is the regular at the origin, hence

$$\mathbf{U}^i(r) = \sum A_n \hat{\boldsymbol{\psi}}_{fn}. \tag{10b}$$

The displacement fields inside the spheroid must be regular at the origin.

$$\mathbf{U}(r)=\sum \alpha_{vn}\psi_{vn}. \tag{10c}$$

The expansion of the Green's function for these basis have been given in Ref. 16 and are repeated as

$$G_f(r,r')=(ik/\rho_f\omega^2)\sum \psi_{fn}(r_>)\hat{\psi}_{fn}(r_<) \tag{11a}$$

and

$$G(r,r')=(ik_s/\rho_f\omega^2)\sum \psi_{in}(r_>)\,\mathrm{Re}\{\psi_{vn}\}(r_<), \tag{11b}$$

where $r_>$ and $r_<$ refer to the greater and lesser of r and r'.

Substituting Eq. (10) into the integral Eq. (6a) and using the boundary conditions, one obtains

$$A_n=-\sum iQ_{n,vn'}\alpha_{vn'} \tag{12a}$$

and

$$f_m=\sum iQ_{n,vn'}\alpha_{vn'}, \tag{12b}$$

where the matrix Q is given by

$$Q_{n,vn'}=\left(\frac{k}{\rho_f\omega^2}\right)\int_S [\lambda_f\nabla\cdot\psi_{fn}\hat{n}\cdot\hat{\psi}_{vn'}-\hat{n}\cdot\psi_{fn}\cdot\mathbf{t}(\hat{\psi}_{vn'})]\,dS'. \tag{13}$$

Due to the summation on v which varies from 1 to 3 the Q matrix has a 1×3 substructure and cannot be inverted. In order to obtain the desired T matrix connecting A_n and f_n we must invoke Eq. (6). Following Bostrom[17] one defines a new expansion for the exterior surface field on S, to obtain a set of matrices that are invertible. We follow Bostrom[17] by defining

$$\mathbf{U}_f(r)=\sum d_n\hat{\psi}_{fn}. \tag{14}$$

Using Eq. (5) for the tangential component of the displacement and all components of stress and using the first two boundary conditions in Eq. (5) we obtain

$$P_{vn,n'}d_{n'}+R_{vn,v'n'}\alpha_{v'n'}=0, \tag{15}$$

where the matrices P and R are given by

$$P_{vn,n'}=\left(\frac{k_s}{\rho\omega^2}\right)\int_S \{(\hat{n}\cdot\hat{\psi}_{fn})[\hat{n}\cdot\mathbf{t}(\hat{\psi}_{fn})]\}\,dS, \tag{16a}$$

$$R_{vn,v'n'}=\left(\frac{k_s}{\rho\omega^2}\right)\int\int \{(\hat{\psi}_{v'n'})\tan g\cdot\mathbf{t}(\hat{\psi}_{vn}) - [\mathbf{t}(\hat{\psi}_{v'n'})]n\cdot\hat{\psi}_{vn}\}\,dS. \tag{16b}$$

From Eqs. (12a), (12b), (15), and (16b) we obtain the following relation between the incident and scattered field coefficients in matrix form,

$$f=TA, \tag{17}$$

where

$$T=-\hat{Q}R^{-1}P(QR^{-1}P)^{-1}. \tag{18}$$

The T matrix defined as Eq. (18) is applicable to any elastic obstacle of arbitrary shape immersed in a fluid.

III. FORM FUNCTION FOR A SPHEROID

From Eqs. (17) and (18) we obtained the scattering coefficient in terms of the T matrix. From Eqs. (10) and (18) the scattered portion of the total acoustic field at a point (r,θ) may be written as

$$U^s=b/2\exp-(i\omega t-kr)f_r, \tag{19}$$

where f_r is the reflected form function given as

$$f_r=2\left(\frac{r}{a}\right)e^{ikr}\sum\sum(-i)^{n+1}h_n(kr)P_n(\cos\theta)\epsilon_{nm}f_{nm}. \tag{20a}$$

For large distances from the reflector, the asymptotic expressions for $h_n(kr)$ in the form function are used with the result that f_r which is now written as f_∞ is expressed

$$f_\infty=\left(\frac{2}{ka}\right)\sum\sum P_n(\cos\theta)f_{nm}. \tag{20b}$$

Equation (20b) describes the reflection characteristics of the spheroid. For monostatic reflection $\theta=\pi$, making $P_n(\cos\theta)=(-1)^n$ and

$$f_\infty=\left(\frac{-2}{ka}\right)\sum_n\sum_{n'}(-1)^n\epsilon_{nm}f_{nm'}. \tag{20c}$$

In order to evaluate numerically the form function (20c), we need to integrate the matrix elements of Q, R, and P, defined in Eqs. (13) and (16), that consist of surface integrals involving the normal and radius vectors.

$$r(\theta,\phi)=[\cos^2\theta/a^2+\sin^2\theta/b^2]^{-1/2}, \tag{21}$$

where $r(\theta,\phi)$ is the radial vector. Using differential geometry one can obtain the normal vector to the surface and hence

$$\hat{n}(\theta)dS=[\hat{e}_r-\hat{e}_\theta/r(\theta)dr(\theta)/d\theta]r^2(\theta)\sin\theta\,d\theta\,d\phi, \tag{22}$$

where $\hat{e}_r$ and $\hat{e}_\theta$ are unit spherical vectors. Note we already made use of azimuthal symmetry and hence all expressions will be independent of the angle ϕ. We will investigate the prolate spheroid case where $a/b>1$.

Using Eqs. (22), (20), and (17) with Gauss–Legendre quadrature integration one can generate the Q, R, and P matrices. The inversion was performed by using Schmidt Orthogonalization techniques and/or Gaussian elimination.

IV. RESONANCE FORMULATION

The resonance theory of acoustic and elastic wave scattering has been described in detail in Refs. 3–6 and shall only be sketched in the present context. This theory demonstrates that resonances from elastic cylinders or spheres are superimposed on a background of reflection resulting from rigid boundary conditions, so that the elastic body can be regarded as a rigid body except in the frequency interval over which the resonance occurs. We rewrite Eqs. (10c) and (17) in terms of the partial waves

$$f_n=\sum_{n'}T_{nn'} \tag{23}$$

$$f_\infty=\sum_n f_n(\pi), \tag{24}$$

which make up the form function. Thus the first few partial waves are

$$f_0 = T_{01} + T_{02} + \ldots T_{0,n},$$
$$f_1 = T_{11} + T_{12} + \ldots T_{1,n}, \tag{25}$$
$$f_2 = T_{21} + T_{22} + \ldots T_{2,n}.$$

When $b/a \to 1$ the integral can be evaluated in closed form and the form function reduces to that of the matrix elements of an elastic sphere in a fluid.

It is now advantageous to consider the rigid spheroid. This is obtained by using Neumann boundary conditions. This condition states that the total field vanishes on S

$$U(r') = 0, \quad r' \text{ on } S, \tag{26}$$

where U is the total field evaluated at the outside surface of the obstacle. If this condition is substituted in Eq. (13) together with the assumed basis function we obtain

$$Q_{\text{rigid}} = \frac{k}{\rho_f \omega^2} \int_S \lambda_f \nabla \cdot \psi_{fn} \hat{n} \cdot \hat{\psi}_{fn'} \, dS. \tag{27}$$

Since there is no shear component in the fluid, Q is a square matrix and can be inverted yielding

$$T = Q\hat{Q}^{-1}. \tag{28}$$

It follows that

$$f^{\text{rigid}} = T^{\text{rigid}} \tag{29a}$$

and

$$f_n - f_n^{\text{rigid}} = \sum_{n'} T_{nn'} - T_{nn'}^{\text{rigid}}. \tag{29b}$$

V. FORM FUNCTION COMPUTATIONS AND COMPARISON WITH RESONANCE PREDICTIONS

Computations of the backscattered form function, for submerged tungsten carbide prolate spheriods, are given in Fig. 2 (a)–(e). The angle of incidence in all five cases is 0° (end on), and the b/a ratio ranges from 0.5 to 0.9. Computations are given over the range $5.0 \lesssim kl/2 \lesssim 10.0$, which covers the range over which the initial departure of the form function from purely rigid body behavior occurs. The description of the scattering by a solid, elastic prolate spheroid conforms to previous elastic scattering descriptions[4] of a rigid body background on to which resonance behavior is superimposed. This is demonstrated in Fig. 3 for the case of a tungsten carbide spheroid with $b/a = 0.5$. The curve seen in Fig. 3 resulted from the term by term subtraction of rigid body partial waves [see Eq. (29)] from the corresponding elastic partial waves. The form function departs from zero only in the region of excitation of the resonance, and as will be discussed below the resonance mechanism is similar to previous observations on spheres and cylinders. Each of the form function curves in Fig. 2 shows the typical rigid body behavior[3-5] at $ka \lesssim 7$ followed by the excitation of a resonance null. The ka position of this initial resonance null can be predicted independently by assuming that the null results from the excitation of a Rayleigh circumferential wave, as was the case for solid elastic cylinders and spheres.[3-5]

The resonance description of acoustic scattering, for metal infinite cylinders, predicted the strong influence

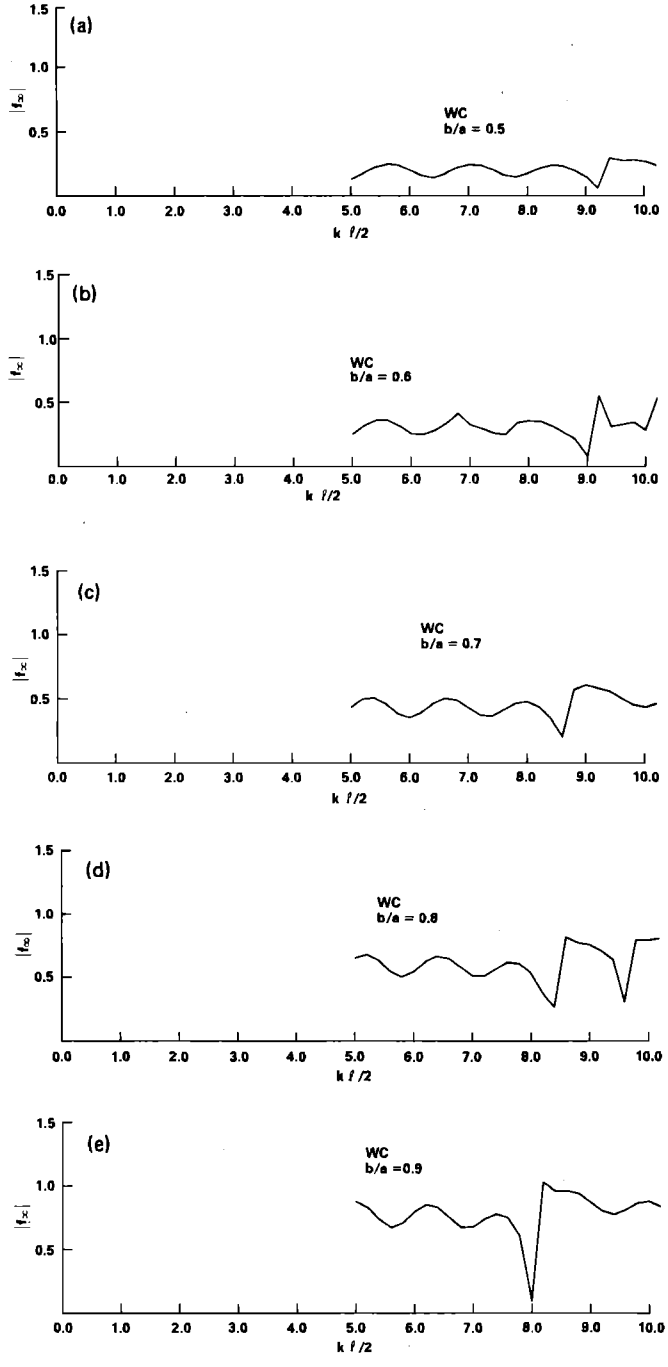

FIG. 2. The form function of a submerged, tungsten carbide, prolate spheroid at end or incidence for b/a values of (a) 0.5, (b) 0.6, (c) 0.7, (d) 0.8, (e) 0.9.

of the Rayleigh surface wave in the target form function, over the range $ka < 20$.[3-5] This prediction was verified by experimental isolation of the surface wave in the expected ka region.[20] The lowest frequency at which resonance behavior is excited for a cylinder occurs when the perimeter of its circular cross section is two Rayleigh wavelengths long or

$$2\pi a = 2\lambda_r = 2c_r/v. \tag{30}$$

From Eq. (30), the ka position $(ka)_{R,1}$ at which the initial resonance occurs for an infinite elastic cylinder is given by

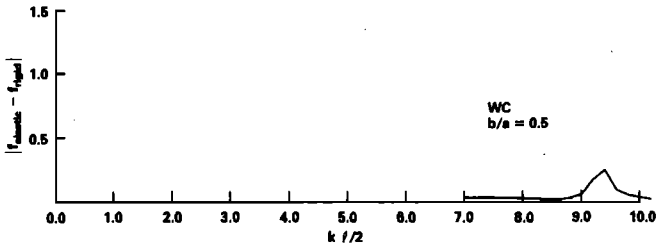

FIG. 3. Term by term subcontraction of rigid body partial waves from elastic partial waves for a tungsten carbide prolate spheroid with $b/a = 0.5$.

$$(ka)_{R,1} = 2(c_r/c). \tag{31}$$

In Eqs. (30) and (31), the c is the speed of sound in water and c_r and λ_r are the Rayleigh speed and Rayleigh wavelength in the target material. The Rayleigh wave is dispersive in this ka region, i.e., c_r has not yet reached its final, flat surface value.[20-23] The resonance is caused by the mutual reinforcement of successive circumnavigations of the Rayleigh wave. Later resonances occur when the cylinder circumference is $n\lambda$, where $n = 3, 4\ldots$; however, for $n > 6$ the attenuation is so large that the effect is insignificant.

The Rayleigh surface wave description also fits the initial resonance in the form function for an elastic sphere. The form function for a tungsten carbide sphere can be computed from a normal mode series solution,[1,24,25] and is given in Fig. 4. The initial departure from a rigid body scattering form function occurs at $(ka)_{R,1} = 7.4$. For a sphere this lowest frequency resonance is also associated with the Rayleigh surface wave[3,4] and occurs at

$$(ka)_{R,1} = \tfrac{5}{2}\, c_r/c. \tag{32}$$

The added factor 1/2 between Eqs. (31) and (32) for the cylinder and sphere is discussed by Uberall.[26]

Until the recent application of the T-matrix approach to elastic boundary value problems, and the extension of these T-matrix computations into the resonance region, no midfrequency analytic computations were possible for finite bodies other than the sphere. It is expected that the Rayleigh wave resonance will also be the initial elastic behavior observed in the form function for other smooth, finite, symmetric targets. If it is assumed that the Rayleigh resonance null occurs in the form function for a prolate spheroid then the following prediction can be made.

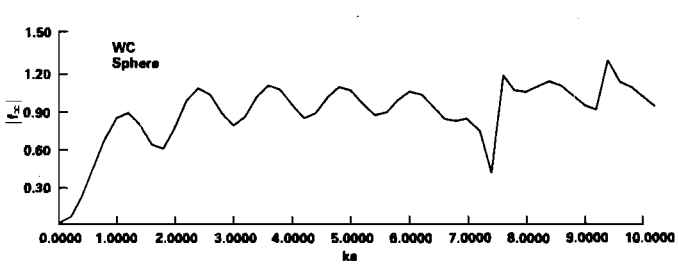

FIG. 4. The form function of a submerged tungsten carbide sphere.

TABLE I. A comparison of null positions predicted from resonance considerations with nulls obtained from the T-matrix computation.

b/a	$(ka)_1$ from geometric considerations	$(ka)_1$ from form functions
0.5	9.6	9.6
0.6	9.1	9.2
0.7	8.7	8.6
0.8	8.2	8.3
0.9	7.8	8.0

Consider a sphere of radius a circumscribed about the spheroid seen in Fig. 1. The form function of both of the targets is defined as

$$f_\infty = (2r/a)(p_r/p_0)(\approx 1 \text{ for a rigid sphere}), \tag{33}$$

where p_r and p_0 are, respectively, the steady-state reflected and incident pressure amplitudes. Based on the their respective cross sections, the rigid body or background form function for the prolate spheroid should be, in general, smaller by a factor b^2/a^2 than that for the circumscribed sphere[27] at end-on incidence. Additionally, if the perimeter of the elliptical cross section ADA in Fig. 1 is given by $P = P_1 a$, then at end on incidence the ka value at which the Rayleigh wave resonance occurs $(ka)_1$ for the spheroid should be related to the corresponding sphere resonance position $(ka)_{R,1}$ (Fig. 4) by

$$(ka)_1 = (2\pi/P_1)(ka)_{R,1}. \tag{34}$$

Table I compares the resonance positions observed in the form functions shown in Fig. 2, and values computed from Eq. (34). The greatest difference is 2.5%.

VI. SUMMARY

The T-matrix formulation allows the computation of the acoustic scattering by submerged, finite targets to be obtained into the mid or resonance frequency range. Computations of the scattering by an elastic prolate spheroid were obtained for the first time by applying the T-matrix method. The resonance nulls occurred at the ka values predicted by resonance considerations.

[1] J. J. Faran, Jr., J. Acoust. Soc. Am. 23, 405 (1951).
[2] R. H. Vogt and W. G. Neubauer, J. Acoust. Soc. Am. 60, 15 (1976).
[3] H. Überall, L. R. Dragonette, and L. Flax, J. Acoust. Soc. Am. 61, 711 (1977).
[4] L. Flax, L. R. Dragonette, and H. Überall, J. Acoust. Soc. Am. 63, 723 (1978).
[5] L. R. Dragonette, Nav. Res. Lab. Rep. 8216 (1978).
[6] L. Flax, G. C. Gaunard, and H. Überall, in *Physical Acoustics*, edited by W. P. Mason and R. N. Thurston (Academic, New York, 1980), Vol. XV.
[7] A. Silbiger, J. Acoust. Soc. Am. 35, 564 (1963).
[8] T. B. A. Senior, Can. J. Phys. 44, 655 (1966).
[9] R. Hickling, J. Acoust. Soc. Am. 30, 137 (1958).
[10] R. D. Spence and S. Granger, J. Acoust. Soc. Am. 23, 701 (1951).
[11] J. E. Burke, J. Acoust. Soc. Am. 40, 325 (1966).
[12] J. E. Burke, J. Acoust. Soc. Am. 39, 826 (1966).

[13]N. G. Gatkin, Sov. Phys.-Acoust. 17, 313 (1972).
[14]P. C. Waterman, J. Acoust. Soc. Am. 60, 567 (1976).
[15]V. Varatharajulu (V.V. Varadan) and Y. H. Pao, J. Acoust. Soc. Am. 60, 556 (1976).
[16]A. Bostrom, J. Acoust. Soc. Am. 67, 390 (1980).
[17]B. A. Peterson, V. V. Varadan, and V. K. Varadan, Int. J. Wave Motion 2, 23 (1980).
[18]J.-H. Su, V. V. Varadan, V. K. Varadan, and L. Flax, J. Acoust. Soc. Am. 68, 686 (1980).
[19]V. K. Varadan, V. V. Varadan, L. R. Dragonette, and L. Flax, J. Acoust. Soc. Am. 71, 22 (1982).
[20]L. R. Dragonette. J. Acoust. Soc. Am. 63 (1979).
[21]G. V. Frish and H. Überall, J. Acoust. Soc. Am. 59, 46 (1976).
[22]J. W. Dickey and H. Überall, J. Acoust. Soc. Am. 59, 46 (1976).
[23]R. D. Doolittle, H. Überall, and P. Ugencius, J. Acoust. Soc. Am. 43, 1 (1968).
[24]R. Hickling, J. Acoust. Soc. Am. 34, 1582 (1962).
[25]W. G. Neubauer, R. H. Vogt, and L. R. Dragonette, J. Acoust. Soc. Am. 55, 1123 (1974).
[26]H. Überall, *Modern Problems in Elastic Wave Propagation*, edited by J. Miklowitz and J. Achenbach (1978).
[27]A. J. Rudgers, J. Acoust. Soc. Am. 39, 294 (1966).